Understanding the Reconstructive Phase Transition in Pb

Physics 492R Capstone Project

Richard Hansen

Advisors: Harold T. Stokes, Dorian M. Hatch, James R. Lewis

Table of Contents

Abstract

We investigate the mechanism responsible for the reconstructive fcc-hcp phase transition in Pb that occurs at about 13 GPa. The two most energetically favorable atomic pathways have enthalpy barriers much lower than any other pathway we considered. Both mechanisms involve only shifts of (111) planes in the fcc structure. We physically interpret these pathways and represent them graphically.

Introduction

Under normal conditions (STP) Pb crystallizes in a face-centered-cubic (fcc) structure with one atom per cell. It was suspected nearly forty years ago that a transition to another structure could be induced by applying pressure, but the pressure of transition and the structure of the new phase was not immediately determined[1]. Balchan and Drickamer were the first to detect the transition, estimating it ensued at 16 GPa and determining the new structure to be hexagonal close-packed (hcp)[2]. More recently it has been estimated that the phase transition occurs at room temperature somewhere between 12-14 GPa. However, as with many other transitions, a large degree of hysteresis could cause both types of structures to exist simultaneously in Pb.

The fcc-hcp transition occurs naturally in many other substances including gold, cobalt, and iron[3]. Two common mechanisms for an fcc-hcp phase transition have been extensively theorized but never observed. The first is known as the Shoji-Nishiyama (SN) mechanism[4]. Others have anticipated this mechanism to be the most common and energetically favorable. In the SN phase transition, pairs of (111) planes move in the

$[1/6\ -1/3\ 1/6]_{fcc}$ direction relative to adjacent pairs of planes. All pairs of planes shift in the same direction. The $[111]_{fcc}$ becomes $[0001]_{hcp}$ in the new hcp structure.

Another mechanism to achieve the fcc-hcp phase transition has been recently proposed by Wentzcovitch *et al.*[5] and has been found to be equally as energetically favorable. In this type of transition, adjacent (001) planes of the fcc structure experience a shear in opposite directions along $[100]_{fcc}$. Then the (001) planes are extended along $[100]_{fcc}$, and compressed along the $[010]_{fcc}$ direction. Thus the total effect the distortions change the (001) planes in the fcc structure to become identical to the (0001) planes in the hcp crystal. This distortion is then followed by a compressive strain in the [001] direction. Therefore, in this alternate mechanism, $[0001]_{hcp}$ is parallel to the initial $[001]_{fcc}$ direction.

The fcc-hcp problem has been extensively researched in the past, some inquiries specifically relating to Pb, although it was not currently clear which mechanism causes this transition in Pb. Our intent is to use COMSUBS, in conjunction with other sophisticated computing programs, as a new approach to answer this difficult question. Dr. Stokes has led several projects similar to this one, including the study of reconstructive phase transitions in Ti[6], NaCl[7], PbS[8], SiC[9].

The ultimate goal for this project was to identify probable atomic pathways in the fcc-hcp phase transition of elemental Pb. The project was executed completely through numerical methods using computers. We have found that our computations and data are in general agreement with physical experiments and other recent literature regarding fcc-hcp transitions. The only significant difference is that we have identified the model proposed by Wentzcovitch *et al.* to not actually be as energetically favorable in the case

of Pb. I believe that through the methods of this project, we have identified the two most energetically favorable, and thus the most likely, atomic pathways of the fcc-hcp transition in Pb. These two pathways are related to each other, and involve shifts by only (111) planes, variations of the SN mechanism.

Computational Methods

The first step in this project was to identify the target parameters and pressure to be used for numerical analysis. The key computer program in this process was FIREBALL[10] which is a program that rapidly calculates the energy of a crystal using first-principle methods. We used FIREBALL to calculate the lattice parameters and total enthalpy for both the fcc and hcp structures at pressures ranging from 0 to 50 GPa. We found that for pressures less than 34 GPa the fcc structure was more stable. At pressures exceeding this value, the hcp structure was more energetically favorable. This discrepancy with the experimentally determined values of 13 GPa at the transition is due to some approximations made by FIREBALL. We also determined the lattice parameters to be 4.5700 angstroms in the $[100]_{fcc}$, $[010]_{fcc}$, $[001]_{fcc}$ directions for the fcc structure, and 3.2280, 3.2280, 5.2470 angstroms respectively for the hcp structure.

Once we had obtained the pressure of the transition, we employed COMSUBS[11,12] to discover how the transition might occur. COMSUBS is a program that finds possible atomic pathways from one given structure to another, in this case, from fcc to hcp. In order to limit the search to probable atomic pathways, we imposed several constraints (see Appendix).

1) We assume that as Pb evolves from fcc to hcp, its intermediate structure along the pathway is well defined at each point. We assume that the intermediate structure has translational symmetry and can be defined using a unit cell. We limited our search to pathways that involved an intermediate structure with a primitive unit cell containing no more than four atoms.
2) The unit cell of the intermediate structure generally changes its size and shape along the pathway. This strain costs energy. We limited the principal values of the strain tensor to values between 0.6 and 1.5. Basically, this allowed macroscopic distances in the fcc structure to contract by no more than 40% and to expand by no more than 50% when making the transition to hcp.
3) Since atoms cannot pass through each other, we discarded pathways where the distance between any pair of atoms was less than 2.6 angstroms anywhere along the pathway. This value is approximately 80% of the distance between nearest neighbors in the fcc structure.
4) Atoms near each other in the fcc structure should also be near each other in the hcp structure. To achieve this, we discarded pathways where the atoms were displaced more than 3.3 angstroms from the center-of-mass position in the unit cell of the intermediate structure.

COMSUBS returned 618 possible atomic pathways for the fcc-hcp transition in Pb. Not all of the solutions, however, are naturally viable. Each individual pathway has a specific enthalpy barrier, and only the solutions with the lowest barriers would ever occur naturally. Thus to determine which paths are most probable for this transition, the enthalpy barriers of each needed to be determined. Using FIREBALL and the

information about the atomic pathways provided by COMSUBS, we can calculate the enthalpy along each pathway from fcc to hcp. If we assume a linear pathway, we obtain an upper limit to the barrier of each case.

We found that the FIREBALL calculations were taking much longer than anticipated. Each pathway required a few hours for FIREBALL to analyze. Because of the large number of pathways, the total expected time to run the full examination for each pathway was estimated to exceed several weeks. For this reason we searched for methods that would either shorten the runtime or further limit the scope of our investigation. We decided to calculate the enthalpy at only the midpoint of each pathway. This midpoint enthalpy of each pathway could underestimate the actual barrier, but we hoped that using this midpoint value we could immediately identify and eliminate pathways with very high enthalpy. This limited runtime to minutes instead of hours. Only pathways with extreme enthalpy asymmetries or local minima would be misrepresented by the calculation. After employing this strategy, six pathways in particular had comparatively very low enthalpy barriers. We decided to proceed with a full investigation of these pathways with the caveat that if none of them produced an actual enthalpy barrier (not just the midpoint value) lower than the midpoint value of any of the other 612 pathways, we would have to expand the investigation upwards. Fortunately, as explained in the ensuing section for results, this did not turn out to be the case.

After narrowing our investigation to just six pathways, we investigated the enthalpy barrier with FIREBALL along each entire pathway. We also removed the

restriction to linear pathways and used the method of bow functions[13] to find the enthalpy at the top of the actual barrier.

Once the final pathways had been determined, we still had to physically interpret the actual movement of the atoms in each pathway. Using the information from COMBSUBS, we could calculate the actual movement of each atom along each pathway. We did this to observe the relative placement of atoms to their nearest neighbors. This is useful for understanding what type of transition is taking place, for example planar shifts or distortions along an axis. There will be a repeatable pattern among unit cells, and we searched for that pattern with the lowest two pathways.

Some pathways were too difficult to interpret on paper, so we had to figure out another means of representing atomic movement. To do this and check our result from more simple pathways, we graphically modeled the transition of the pathways in MATLAB, a powerful numeric mathematics computer program. We were able to use MATLAB to render a three dimensional model of the actual movement of the atoms. This process could be applied to any transition given the pathway information from COMSUBS. MATLAB verified our results and helped us visualize an important relationship between the two lowest pathways.

Results

FIREBALL found the approximate pressure of the phase transition to be 34 GPa. For time considerations as discussed above, only the enthalpy barrier at the midpoint of each atomic pathway was calculated. This was used merely as an approximation to narrow the scope of investigation. COMSUBS returned 618 possible atomic pathways

that met the required constraints. The midpoint enthalpy values of the pathways resemble a bell curve on the histogram depicted below.

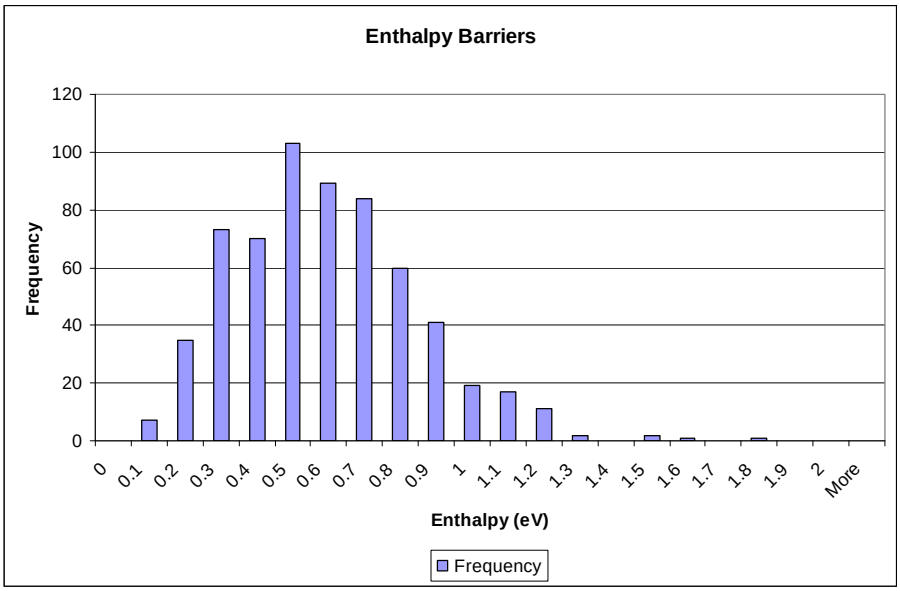

Fig. 1: Histogram of enthalpy at the midpoint of the 618 pathways returned by COMSUBS

Only those with the lowest enthalpy values are likely to occur naturally and so are the only pathways considered. Figure 2 shows the histogram of only the pathways with the seven lowest midpoint enthalpy values.

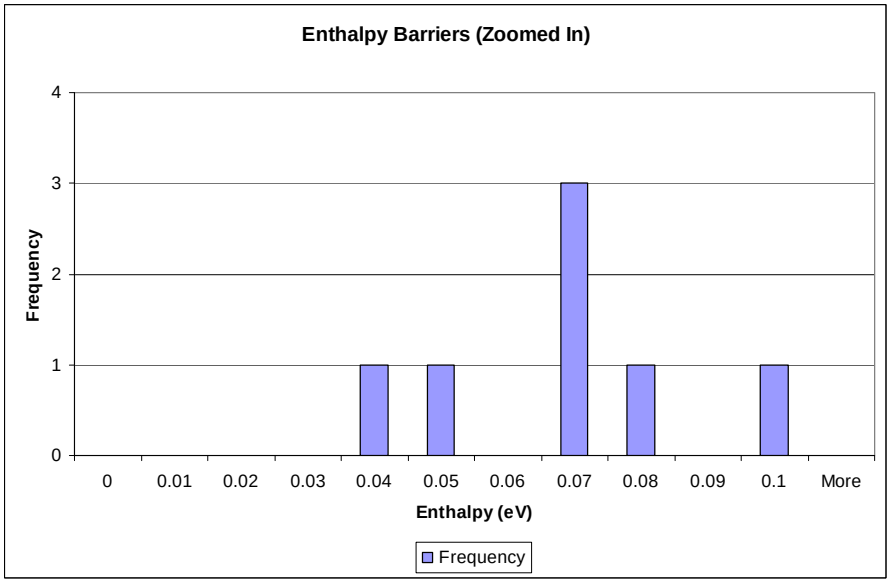

Fig. 2: Histogram of enthalpy at the midpoint of the 7 lowest pathways

Of the 618 pathways, cases 3, 11, 416, 468, 484 and 501 had the lowest enthalpy values at the midpoint of transition, and are thus the pathways of interest. We used the bow function method with FIREBALL to calculate the actual enthalpy barrier. Results are shown in Fig. 3 and 4 below.

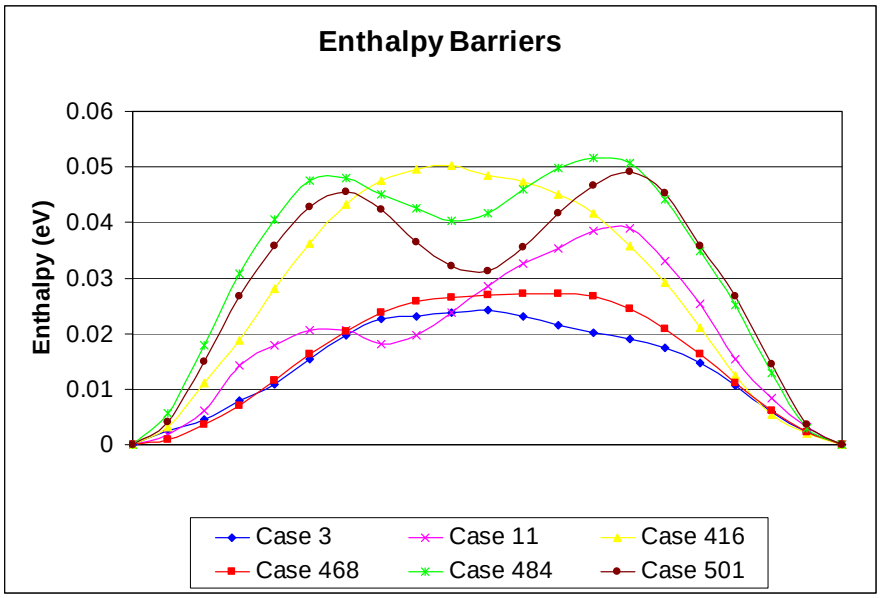

Fig. 3: Actual enthalpy barriers for the six lowest pathways.

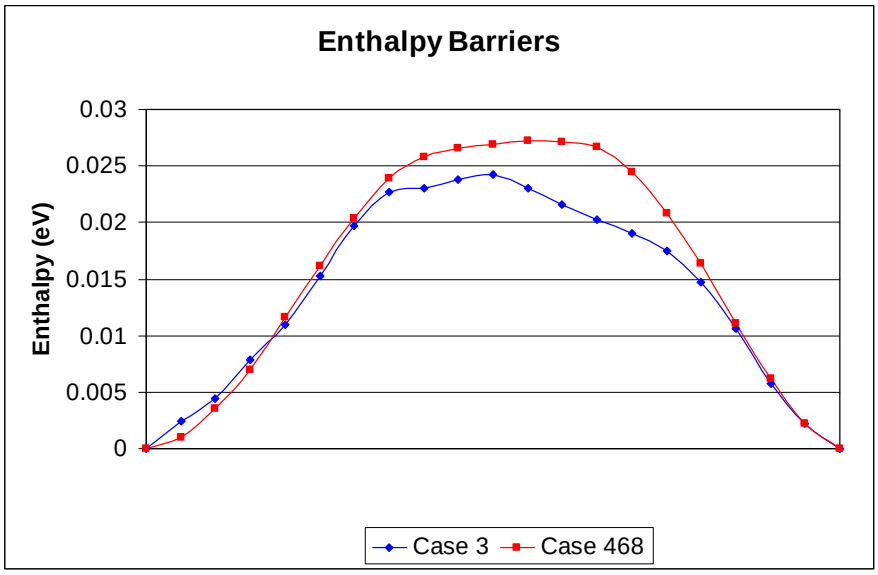

Fig. 4: Actual enthalpy barriers for the two lowest pathways.

As depicted in Fig. 3, the actual enthalpy barriers of the 3rd and 4th lowest pathways were actually comparatively much higher than the midpoint prediction, thus narrowing the relevant investigation to cases 3 and 468 only. Importantly, the midpoint enthalpy value strategy initially employed to speed up the analysis did in fact return the most energetically favorable pathways since the actual enthalpy barriers for these two pathways were indeed lower than the midpoint value of any other pathway.

Discussion of Results

FIREBALL identified the two pathways with the lowest enthalpy barrier. To further investigate the actual mechanism of these two pathways, we used MATLAB to create a three dimensional representation of the actual movement of individual atoms and planes of atoms. We wrote a MATLAB script that used the information from COMSUBS to calculate the end position of an atom, given an initial reference point. From this modeling, it became apparent that the two lowest atomic pathways for Pb were of the SN mechanism variety. Interestingly, cases 3 and 468 experienced only shifts of (111) planes and no distortions. These pathways are related in the sense that only planar shifts, and relatively short ones, are involved. However, case 3 involves planar shifts in only a single direction, while case 468 uses planar shifts along two directions to accomplish the same transition. Because both pathways use shifts only along the (111) plane, two-dimensional representations, although slightly less effective than the MATLAB three-dimensional models, are adequate to illustrate the atomic movement of the planes.

Case 3 represents the most simple fcc-hcp transition. This transition involves (111) planar shifts in the same direction. As seen in figures in the appendix, atoms in the same (111) plane create a pocket in the shape of an equilateral triangle. Each (111) plane effectively sits in such pockets of the planes directly above and below. During this transition, pairs of planes move together, shifting to an adjacent pocket of the top plane of the pair directly beneath. This pattern of shifting relative to the pair of planes directly beneath repeats throughout the entire crystal.

Although case 468 also exclusively uses shifts of the (111) planes, the process is slightly more complicated. All planes do not move in the same direction. However, the two different planar shifts together effectively creates the same result as in case 3. Like case 3, the first pair of planes move to an adjacent pocket between atoms of the plane directly beneath. The next pair of planes on top, however, moves in a different direction, but still to an adjacent pocket (see Appendix).

Conclusions

Our calculations using COMSUBS and FIREBALL has reasonably demonstrated that planar shifts are the most energetically advantageous mechanism for the fcc-hcp transition in Pb. Compared to the rest of the pathways, the (111) planar shifts are a very simple mechanism. This simplicity could be a reason for very little strain in the crystal, as well as simple enthalpy barriers for cases 3 and 468. It also naturally leads to the assumption that these planar shifts from pocket to pocket have a low energy barrier in general. Two of the other six lowest pathways, cases 484 and 501, were mechanisms of longer planar shifts between pockets as well.

The Wentzcovitch *et al.* mechanism in Pb did not appear in the lowest group of atomic pathways, and we were not able to identify which of the 618 pathways represented this mechanism so we cannot conjecture how much higher its enthalpy barrier is. It is still plausible this alternate mechanism may be preferable in other materials.

Appendix

fcc and hcp Structures

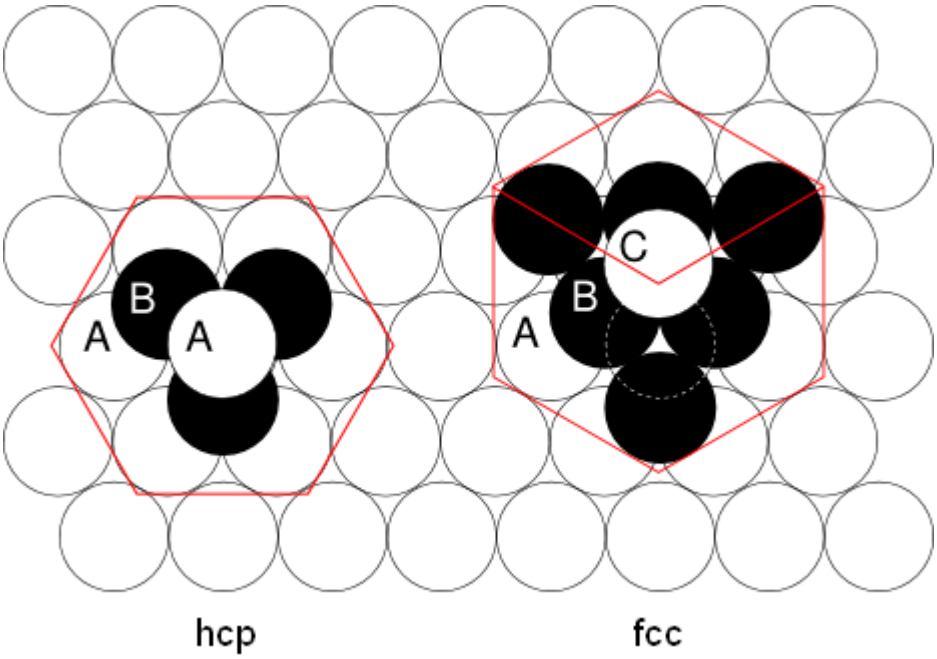

fcc Structure

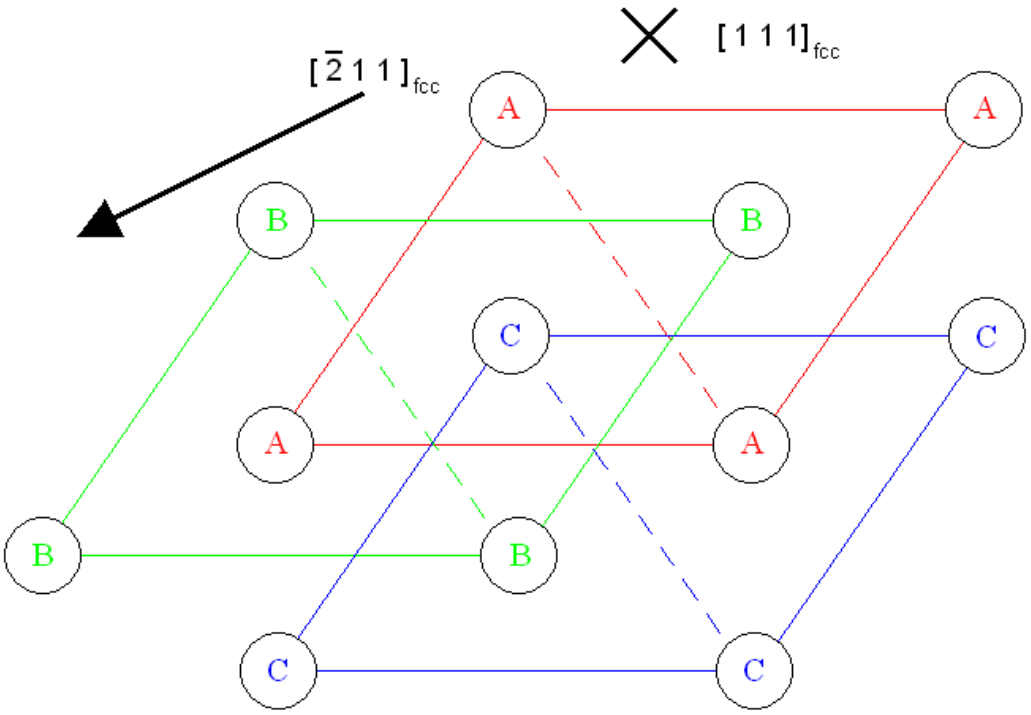

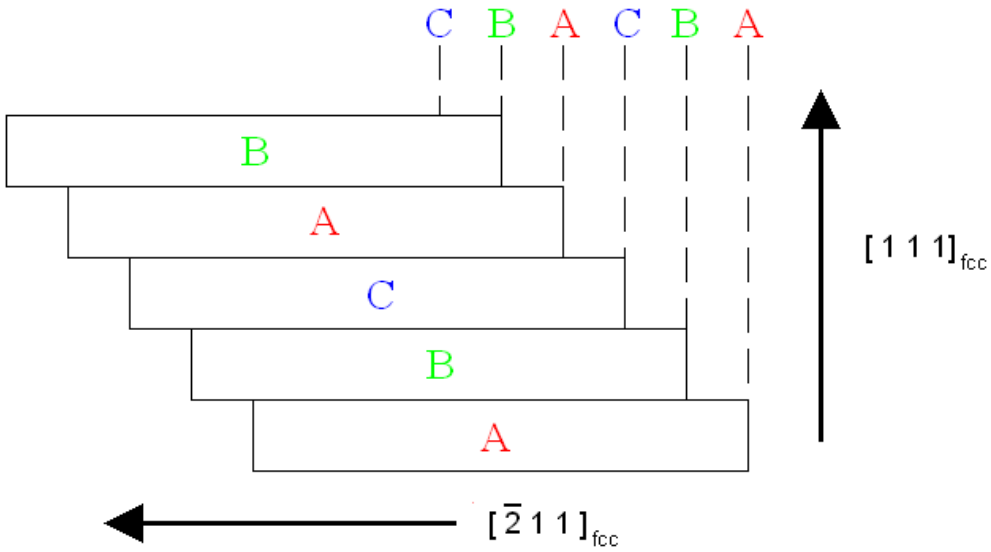

hcp Structure

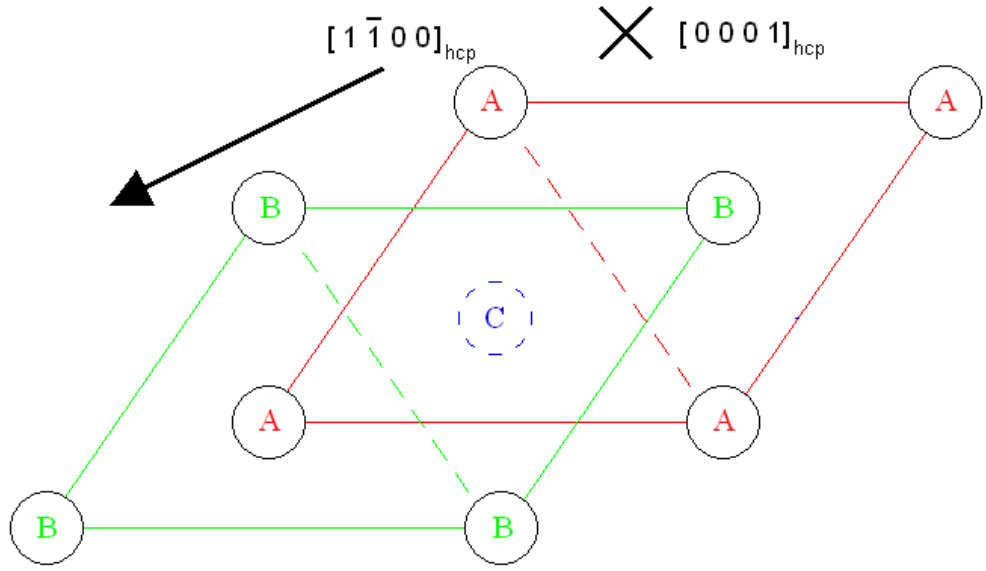

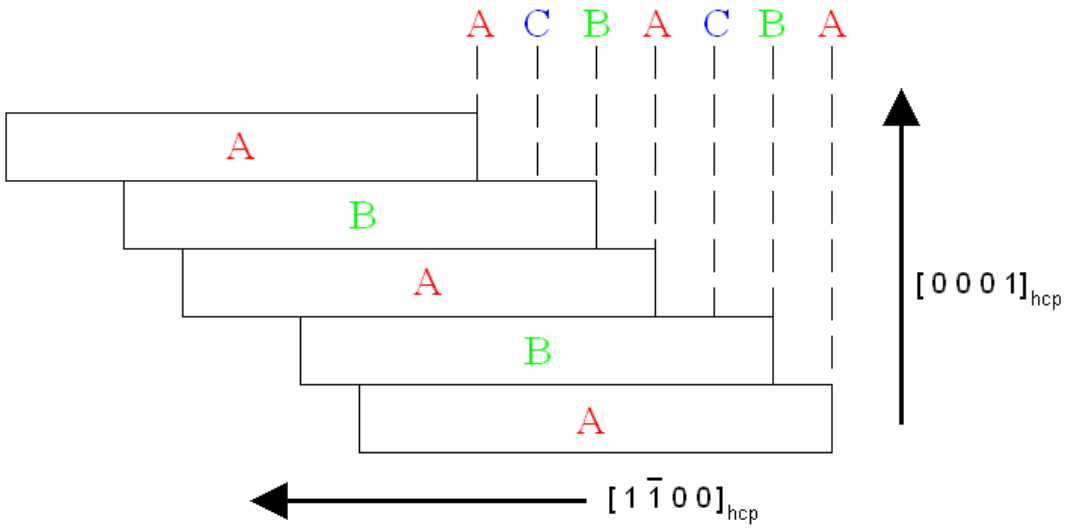

COMSUBS Input

```
comsubs, version 2.1.1, July 2004
Harold T. Stokes and Dorian M. Hatch, Brigham Young University
Thu Feb 17 09:41:31 2005

Pb fcc to hcp
First crystal:
        Space group: 225 Fm-3m
        Lattice parameters:    4.5700   4.5700   4.5700  90.0000  90.0000  90.0000
        Number of Wyckoff positions:   1
        Pb, Wyckoff position a,    0.00000   0.00000   0.00000
Second crystal:
        Space group: 194 P6_3/mmc
        Lattice parameters:    3.2280   3.2280   5.2470  90.0000  90.0000 120.0000
        Number of Wyckoff positions:   1
        Pb, Wyckoff position c,    0.33333   0.66667   0.25000
Minimum size of unit cell:   2
Maximum size of unit cell:   4
Minimum strain: .600
Maximum strain: 1.50
Constrain shuffle to  3.30
Minimum distance between atoms:    2.600
Use fireball to estimate energy barrier
Number of atoms in primitive unit cell of crystal 1:   1
Number of atoms in primitive unit cell of crystal 2:   2
Volume/atom in crystal 1:     23.861
Volume/atom in crystal 2:     23.674
Nearest distance between atoms in crystal 1:    3.2315
Nearest distance between atoms in crystal 2:    3.2181
```

COMSUBS Output for Cases 3 and 468

Case 3

Principal values of strain tensor: 1.189 0.999 0.836
Nearest-neighbor distance along path: 3.148
Broken bonds: 1 out of 18
Maximum atomic shuffle: 0.466
Common subgroup: 12 C2/m
Setting of crystal 1:
Size = 2
Lattice: (1,-1/2,-1/2),(0,1/2,-1/2),(0,1,1)
Origin: (0,1/4,1/4)
Lattice parameters: 5.5971 3.2315 6.4630 90.0000 125.2644 90.0000
Pb i x'= 0.00000, z'= 0.75000
Setting of crystal 2:
Size = 1
Lattice: (2,1,0),(0,-1,0),(-2,-1,-1)
Origin: (-1,-1/2,-1)
Lattice parameters: 5.5911 3.2280 7.6675 90.0000 136.8183 90.0000
Pb i x'=-0.08333, z'= 0.75000
At midpoint:
Lattice parameters: 5.5706 3.2162 7.0356 90.0000 131.0413 90.0000
Pb i x'=-0.04167, z'= 0.75000
Estimated energy barrier using fireball: 0.050 eV

Case 468

Principal values of strain tensor: 1.089 0.999 0.912
Nearest-neighbor distance along path: 3.102
Broken bonds: 2 out of 36
Maximum atomic shuffle: 0.841
Common subgroup: 15 C2/c
Setting of crystal 1:
Size = 4
Lattice: (1/2,1/2,-1),(-1/2,1/2,0),(1,1,2)
Origin: (-1/4,1/4,1/2)
Lattice parameters: 5.5971 3.2315 11.1942 90.0000 109.4712 90.0000
Pb f x'= 0.25000, y'= 0.50000, z'= 0.87500
Setting of crystal 2:
Size = 2
Lattice: (2,1,0),(0,-1,0),(-2,-1,-2)
Origin: (-3/2,-1,-2)
Lattice parameters: 5.5911 3.2280 11.8905 90.0000 118.0481 90.0000
Pb f x'= 0.29167, y'= 0.75000, z'= 0.87500
At midpoint:
Lattice parameters: 5.5870 3.2257 11.5277 90.0000 113.7597 90.0000
Pb f x'= 0.27083, y'= 0.62500, z'= 0.87500
Estimated energy barrier using fireball: 0.038 eV

MATLAB Inputs

```
% Subgroup 3

clear;clc;close all;


% Form arrays
xa=zeros(size(7));
ya=zeros(size(7));
za=zeros(size(7));

xb=zeros(size(7));
yb=zeros(size(7));
zb=zeros(size(7));

xc=zeros(size(7));
yc=zeros(size(7));
zc=zeros(size(7));


xah=zeros(size(7));
yah=zeros(size(7));
zah=zeros(size(7));

xbh=zeros(size(7));
ybh=zeros(size(7));
zbh=zeros(size(7));

xch=zeros(size(7));
ych=zeros(size(7));
zch=zeros(size(7));


xaf=zeros(size(7));
yaf=zeros(size(7));
zaf=zeros(size(7));

xbf=zeros(size(7));
ybf=zeros(size(7));
zbf=zeros(size(7));

xcf=zeros(size(7));
ycf=zeros(size(7));
zcf=zeros(size(7));

% Planes in hexagonal coords.
% 1st plane
xa(1)=0;
ya(1)=0;
za(1)=0;

xb(1)=0;
yb(1)=1;
zb(1)=0;

xc(1)=1;
yc(1)=1;
zc(1)=0;

% 2nd plane
xa(2)=1/3;
ya(2)=2/3;
za(2)=1/2;

xb(2)=1/3;
yb(2)=5/3;
zb(2)=1/2;
```

```
xc(2)=4/3;
yc(2)=5/3;
zc(2)=1/2;

% 3rd plane
xa(3)=0;
ya(3)=0;
za(3)=1;

xb(3)=0;
yb(3)=1;
zb(3)=1;

xc(3)=1;
yc(3)=1;
zc(3)=1;


% 4th plane
xa(4)=1/3;
ya(4)=2/3;
za(4)=1/2+1;

xb(4)=1/3;
yb(4)=5/3;
zb(4)=1/2+1;

xc(4)=4/3;
yc(4)=5/3;
zc(4)=1/2+1;

% 5th plane
xa(5)=0;
ya(5)=0;
za(5)=2;

xb(5)=0;
yb(5)=1;
zb(5)=2;

xc(5)=1;
yc(5)=1;
zc(5)=2;


% 6th plane
xa(6)=1/3;
ya(6)=2/3;
za(6)=1/2+2;

xb(6)=1/3;
yb(6)=5/3;
zb(6)=1/2+2;

xc(6)=4/3;
yc(6)=5/3;
zc(6)=1/2+2;

% 7th plane
xa(7)=0;
ya(7)=0;
za(7)=3;

xb(7)=0;
yb(7)=1;
zb(7)=3;

xc(7)=1;
yc(7)=1;
zc(7)=3;
```

```
% Transform into fcc
n=1;
while n<8

    % 1st & 2nd steps
    xah(n)=.5*xa(n)-za(n)-1/12;
    yah(n)=.5*xa(n)-ya(n);
    zah(n)=-za(n)+3/4;

    xbh(n)=.5*xb(n)-zb(n)-1/12;
    ybh(n)=.5*xb(n)-yb(n);
    zbh(n)=-zb(n)+3/4;

    xch(n)=.5*xc(n)-zc(n)-1/12;
    ych(n)=.5*xc(n)-yc(n);
    zch(n)=-zc(n)+3/4;

    % 3rd step
    if ((zah(n)==(3/4)) | zah(n)==(-1/4) | zah(n)==(7/4) | zah(n)==(11/4) |
zah(n)==(15/4))
        xah(n)=xah(n)+1/12;
        1
    end

    if (zah(n)==(1/4) | zah(n)==(-3/4) | zah(n)==(5/4) | zah(n)==(9/4) | zah(n)==(13/4))
        xah(n)=xah(n)-1/12;
        2
    end

    if (zbh(n)==(3/4) | zbh(n)==(-1/4) | zbh(n)==(7/4) | zbh(n)==(11/4) | zbh(n)==(15/4))
        xbh(n)=xbh(n)+1/12;
        3
    end

    if (zbh(n)==(1/4) | zbh(n)==(-3/4) | zbh(n)==(5/4) | zbh(n)==(9/4) | zbh(n)==(13/4))
        xbh(n)=xbh(n)-1/12;
        4
    end

    if (zch(n)==(3/4) | zch(n)==(-1/4) | zch(n)==(7/4) | zch(n)==(11/4) | zch(n)==(15/4))
        xch(n)=xch(n)+1/12;
        5
    end

    if (zch(n)==(1/4) | zch(n)==(-3/4) | zch(n)==(5/4) | zch(n)==(9/4) | zch(n)==(13/4))
        xch(n)=xch(n)-1/12;
        6
    end

    % 4th step
    zah(n)=zah(n)-3/4;
    zbh(n)=zbh(n)-3/4;
    zch(n)=zch(n)-3/4;

    % 5th step (last)
    xaf(n)=xah(n);
    yaf(n)=-.5*xah(n)+.5*yah(n)+zah(n);
    zaf(n)=-.5*xah(n)-.5*yah(n)+zah(n);

    xbf(n)=xbh(n);
    ybf(n)=-.5*xbh(n)+.5*ybh(n)+zbh(n);
    zbf(n)=-.5*xbh(n)-.5*ybh(n)+zbh(n);

    xcf(n)=xch(n);
    ycf(n)=-.5*xch(n)+.5*ych(n)+zch(n);
    zcf(n)=-.5*xch(n)-.5*ych(n)+zch(n);

    % Increment
    n=n+1;
end
```

```
% [111] line for orientation purposes
xline = -4:.1:4;
yline = -4:.1:4;
zline = -4:.1:4;


plot3(xaf(1),yaf(1),zaf(1),'rh',xbf(1),ybf(1),zbf(1),'rs',xcf(1),ycf(1),zcf(1),'rx');
hold on
plot3(xaf(2),yaf(2),zaf(2),'bh',xbf(2),ybf(2),zbf(2),'bs',xcf(2),ycf(2),zcf(2),'bx');
hold on
plot3(xaf(3),yaf(3),zaf(3),'gh',xbf(3),ybf(3),zbf(3),'gs',xcf(3),ycf(3),zcf(3),'gx');
hold on
plot3(xaf(4),yaf(4),zaf(4),'ch',xbf(4),ybf(4),zbf(4),'cs',xcf(4),ycf(4),zcf(4),'cx');
hold on
plot3(xaf(5),yaf(5),zaf(5),'kh',xbf(5),ybf(5),zbf(5),'ks',xcf(5),ycf(5),zcf(5),'kx');
hold on
plot3(xaf(6),yaf(6),zaf(6),'mh',xbf(6),ybf(6),zbf(6),'ms',xcf(6),ycf(6),zcf(6),'mx');
hold on
plot3(xaf(7),yaf(7),zaf(7),'yh',xbf(7),ybf(7),zbf(7),'ys',xcf(7),ycf(7),zcf(7),'yx');
hold on
plot3(xline,yline,zline,'k');
```

% Subgroup 468

```
clear;clc;close all;


% Form arrays
xa=zeros(size(9));
ya=zeros(size(9));
za=zeros(size(9));

xb=zeros(size(9));
yb=zeros(size(9));
zb=zeros(size(9));

xc=zeros(size(9));
yc=zeros(size(9));
zc=zeros(size(9));


xah=zeros(size(9));
yah=zeros(size(9));
zah=zeros(size(9));

xbh=zeros(size(9));
ybh=zeros(size(9));
zbh=zeros(size(9));

xch=zeros(size(9));
ych=zeros(size(9));
zch=zeros(size(9));


xaf=zeros(size(9));
yaf=zeros(size(9));
zaf=zeros(size(9));

xbf=zeros(size(9));
ybf=zeros(size(9));
zbf=zeros(size(9));

xcf=zeros(size(9));
ycf=zeros(size(9));
zcf=zeros(size(9));
```

```
% Planes in hexagonal coords.
% 1st plane
xa(1)=0;
ya(1)=0;
za(1)=0;

xb(1)=0;
yb(1)=1;
zb(1)=0;

xc(1)=1;
yc(1)=1;
zc(1)=0;

% 2nd plane
xa(2)=1/3;
ya(2)=2/3;
za(2)=1/2;

xb(2)=1/3;
yb(2)=5/3;
zb(2)=1/2;

xc(2)=4/3;
yc(2)=5/3;
zc(2)=1/2;

% 3rd plane
xa(3)=0;
ya(3)=0;
za(3)=1;

xb(3)=0;
yb(3)=1;
zb(3)=1;

xc(3)=1;
yc(3)=1;
zc(3)=1;


% 4th plane
xa(4)=1/3;
ya(4)=2/3;
za(4)=1/2+1;

xb(4)=1/3;
yb(4)=5/3;
zb(4)=1/2+1;

xc(4)=4/3;
yc(4)=5/3;
zc(4)=1/2+1;

% 5th plane
xa(5)=0;
ya(5)=0;
za(5)=2;

xb(5)=0;
yb(5)=1;
zb(5)=2;

xc(5)=1;
yc(5)=1;
zc(5)=2;


% 6th plane
xa(6)=1/3;
ya(6)=2/3;
```

```
za(6)=1/2+2;

xb(6)=1/3;
yb(6)=5/3;
zb(6)=1/2+2;

xc(6)=4/3;
yc(6)=5/3;
zc(6)=1/2+2;

% 7th plane
xa(7)=0;
ya(7)=0;
za(7)=3;

xb(7)=0;
yb(7)=1;
zb(7)=3;

xc(7)=1;
yc(7)=1;
zc(7)=3;

% 8th plane
xa(8)=1/3;
ya(8)=2/3;
za(8)=1/2+3;

xb(8)=1/3;
yb(8)=5/3;
zb(8)=1/2+3;

xc(8)=4/3;
yc(8)=5/3;
zc(8)=1/2+3;

% 9th plane
xa(9)=0;
ya(9)=0;
za(9)=4;

xb(9)=0;
yb(9)=1;
zb(9)=4;

xc(9)=1;
yc(9)=1;
zc(9)=4;


% Transform into fcc
n=1;
while n<10

    % 1st & 2nd steps
    xah(n)=.5*xa(n)-.5*za(n)+7/24;
    yah(n)=.5*xa(n)-ya(n)+.75;
    zah(n)=-.5*za(n)+.875;

    xbh(n)=.5*xb(n)-.5*zb(n)+7/24;
    ybh(n)=.5*xb(n)-yb(n)+.75;
    zbh(n)=-.5*zb(n)+.875;

    xch(n)=.5*xc(n)-.5*zc(n)+7/24;
    ych(n)=.5*xc(n)-yc(n)+.75;
    zch(n)=-.5*zc(n)+.875;

    % 3rd step
    % a
    if (zah(n)==(7/8) | zah(n)==(7/8+1) | zah(n)==(7/8+2) | zah(n)==(7/8+3) |
zah(n)==(7/8-1) | zah(n)==(7/8-2) | zah(n)==(7/8-3) | zah(n)==(7/8-4))
```

```
        xah(n)=xah(n)-1/24;
        yah(n)=yah(n)-1/4;
    end

    if (zah(n)==(-7/8) | zah(n)==(-7/8+1) | zah(n)==(-7/8+2) | zah(n)==(-7/8+3) |
zah(n)==(-7/8-1) | zah(n)==(-7/8-2) | zah(n)==(-7/8-3) | zah(n)==(-7/8-4))
        xah(n)=xah(n)+1/24;
        yah(n)=yah(n)+1/4;
    end

    if (zah(n)==(3/8) | zah(n)==(3/8+1) | zah(n)==(3/8+2) | zah(n)==(3/8+3) |
zah(n)==(3/8-1) | zah(n)==(3/8-2) | zah(n)==(3/8-3) | zah(n)==(3/8-4))
        xah(n)=xah(n)-1/24;
        yah(n)=yah(n)+1/4;
    end

    if (zah(n)==(-3/8) | zah(n)==(-3/8+1) | zah(n)==(-3/8+2) | zah(n)==(-3/8+3) |
zah(n)==(-3/8-1) | zah(n)==(-3/8-2) | zah(n)==(-3/8-3) | zah(n)==(-3/8-4))
        xah(n)=xah(n)+1/24;
        yah(n)=yah(n)-1/4;
    end

    % b
    if (zbh(n)==(7/8) | zbh(n)==(7/8+1) | zbh(n)==(7/8+2) | zbh(n)==(7/8+3) |
zbh(n)==(7/8-1) | zbh(n)==(7/8-2) | zbh(n)==(7/8-3) | zbh(n)==(7/8-4))
        xbh(n)=xbh(n)-1/24;
        ybh(n)=ybh(n)-1/4;
    end

    if (zbh(n)==(-7/8) | zbh(n)==(-7/8+1) | zbh(n)==(-7/8+2) | zbh(n)==(-7/8+3) |
zbh(n)==(-7/8-1) | zbh(n)==(-7/8-2) | zbh(n)==(-7/8-3) | zbh(n)==(-7/8-4))
        xbh(n)=xbh(n)+1/24;
        ybh(n)=ybh(n)+1/4;
    end

    if (zbh(n)==(3/8) | zbh(n)==(3/8+1) | zbh(n)==(3/8+2) | zbh(n)==(3/8+3) |
zbh(n)==(3/8-1) | zbh(n)==(3/8-2) | zbh(n)==(3/8-3) | zbh(n)==(3/8-4))
        xbh(n)=xbh(n)-1/24;
        ybh(n)=ybh(n)+1/4;
    end

    if (zbh(n)==(-3/8) | zbh(n)==(-3/8+1) | zbh(n)==(-3/8+2) | zbh(n)==(-3/8+3) |
zbh(n)==(-3/8-1) | zbh(n)==(-3/8-2) | zbh(n)==(-3/8-3) | zbh(n)==(-3/8-4))
        xbh(n)=xbh(n)+1/24;
        ybh(n)=ybh(n)-1/4;
    end

    % c
    if (zch(n)==(7/8) | zch(n)==(7/8+1) | zch(n)==(7/8+2) | zch(n)==(7/8+3) |
zch(n)==(7/8-1) | zch(n)==(7/8-2) | zch(n)==(7/8-3) | zch(n)==(7/8-4))
        xch(n)=xch(n)-1/24;
        ych(n)=ych(n)-1/4;
    end

    if (zch(n)==(-7/8) | zch(n)==(-7/8+1) | zch(n)==(-7/8+2) | zch(n)==(-7/8+3) |
zch(n)==(-7/8-1) | zch(n)==(-7/8-2) | zch(n)==(-7/8-3) | zch(n)==(-7/8-4))
        xch(n)=xch(n)+1/24;
        ych(n)=ych(n)+1/4;
    end

    if (zch(n)==(3/8) | zch(n)==(3/8+1) | zch(n)==(3/8+2) | zch(n)==(3/8+3) |
zch(n)==(3/8-1) | zch(n)==(3/8-2) | zch(n)==(3/8-3) | zch(n)==(3/8-4))
        xch(n)=xch(n)-1/24;
        ych(n)=ych(n)+1/4;
    end

    if (zch(n)==(-3/8) | zch(n)==(-3/8+1) | zch(n)==(-3/8+2) | zch(n)==(-3/8+3) |
zch(n)==(-3/8-1) | zch(n)==(-3/8-2) | zch(n)==(-3/8-3) | zch(n)==(-3/8-4))
        xch(n)=xch(n)+1/24;
        ych(n)=ych(n)-1/4;
    end
```

```
    % 4th step
    xah(n)=xah(n)-1/4;
    yah(n)=yah(n)-1/2;
    zah(n)=zah(n)-7/8;

    xbh(n)=xbh(n)-1/4;
    ybh(n)=ybh(n)-1/2;
    zbh(n)=zbh(n)-7/8;

    xch(n)=xch(n)-1/4;
    ych(n)=ych(n)-1/2;
    zch(n)=zch(n)-7/8;

    % 5th step (last)
    xaf(n)=.5*xah(n)-.5*yah(n)+zah(n);
    yaf(n)=.5*xah(n)+.5*yah(n)+zah(n);
    zaf(n)=-xah(n)+2*zah(n);

    xbf(n)=.5*xbh(n)-.5*ybh(n)+zbh(n);
    ybf(n)=.5*xbh(n)+.5*ybh(n)+zbh(n);
    zbf(n)=-xbh(n)+2*zbh(n);

    xcf(n)=.5*xch(n)-.5*ych(n)+zch(n);
    ycf(n)=.5*xch(n)+.5*ych(n)+zch(n);
    zcf(n)=-xch(n)+2*zch(n);

    % Increment
    n=n+1;
end

% [111] line for orientation purposes
xline = -4:.1:4;
yline = -4:.1:4;
zline = -4:.1:4;


plot3(xaf(1),yaf(1),zaf(1),'rh',xbf(1),ybf(1),zbf(1),'rs',xcf(1),ycf(1),zcf(1),'rx');
hold on
plot3(xaf(2),yaf(2),zaf(2),'bh',xbf(2),ybf(2),zbf(2),'bs',xcf(2),ycf(2),zcf(2),'bx');
hold on
plot3(xaf(3),yaf(3),zaf(3),'gh',xbf(3),ybf(3),zbf(3),'gs',xcf(3),ycf(3),zcf(3),'gx');
hold on
plot3(xaf(4),yaf(4),zaf(4),'ch',xbf(4),ybf(4),zbf(4),'cs',xcf(4),ycf(4),zcf(4),'cx');
hold on
plot3(xaf(5),yaf(5),zaf(5),'kh',xbf(5),ybf(5),zbf(5),'ks',xcf(5),ycf(5),zcf(5),'kx');
hold on
plot3(xaf(6),yaf(6),zaf(6),'rp',xbf(6),ybf(6),zbf(6),'rd',xcf(6),ycf(6),zcf(6),'ro');
hold on
plot3(xaf(7),yaf(7),zaf(7),'bp',xbf(7),ybf(7),zbf(7),'bd',xcf(7),ycf(7),zcf(7),'bo');
hold on
plot3(xaf(8),yaf(8),zaf(8),'gp',xbf(8),ybf(8),zbf(8),'gd',xcf(8),ycf(8),zcf(8),'go');
hold on
plot3(xaf(9),yaf(9),zaf(9),'cp',xbf(9),ybf(9),zbf(9),'cd',xcf(9),ycf(9),zcf(9),'co');
hold on
plot3(xline,yline,zline,'k');
```

Pathway 3 Transition

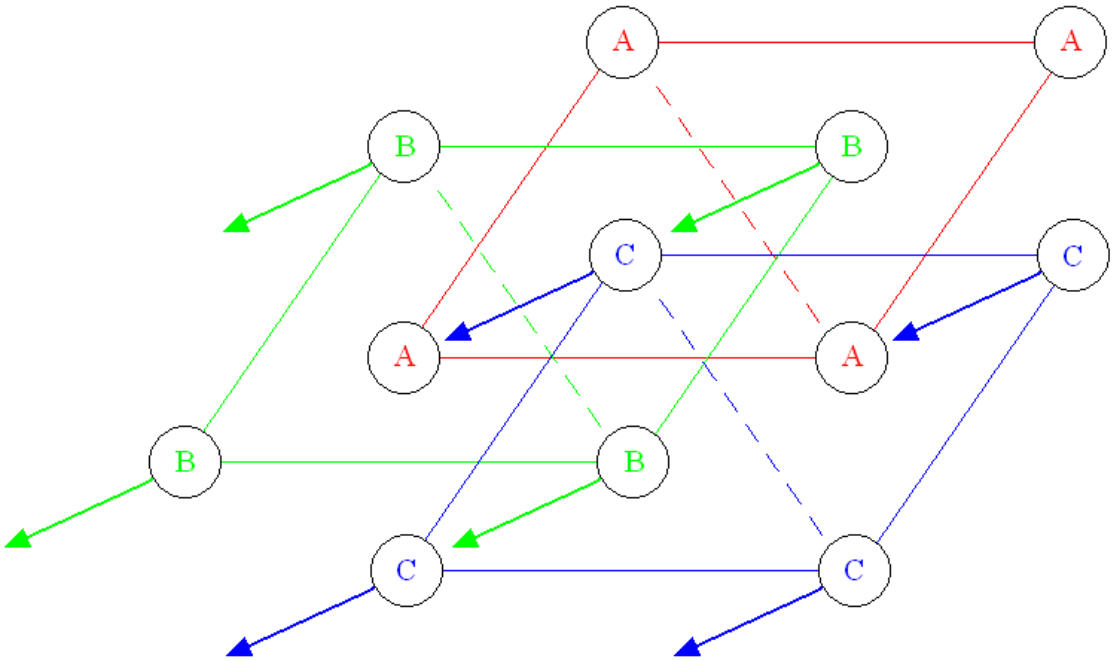

Pathway 3 Transition

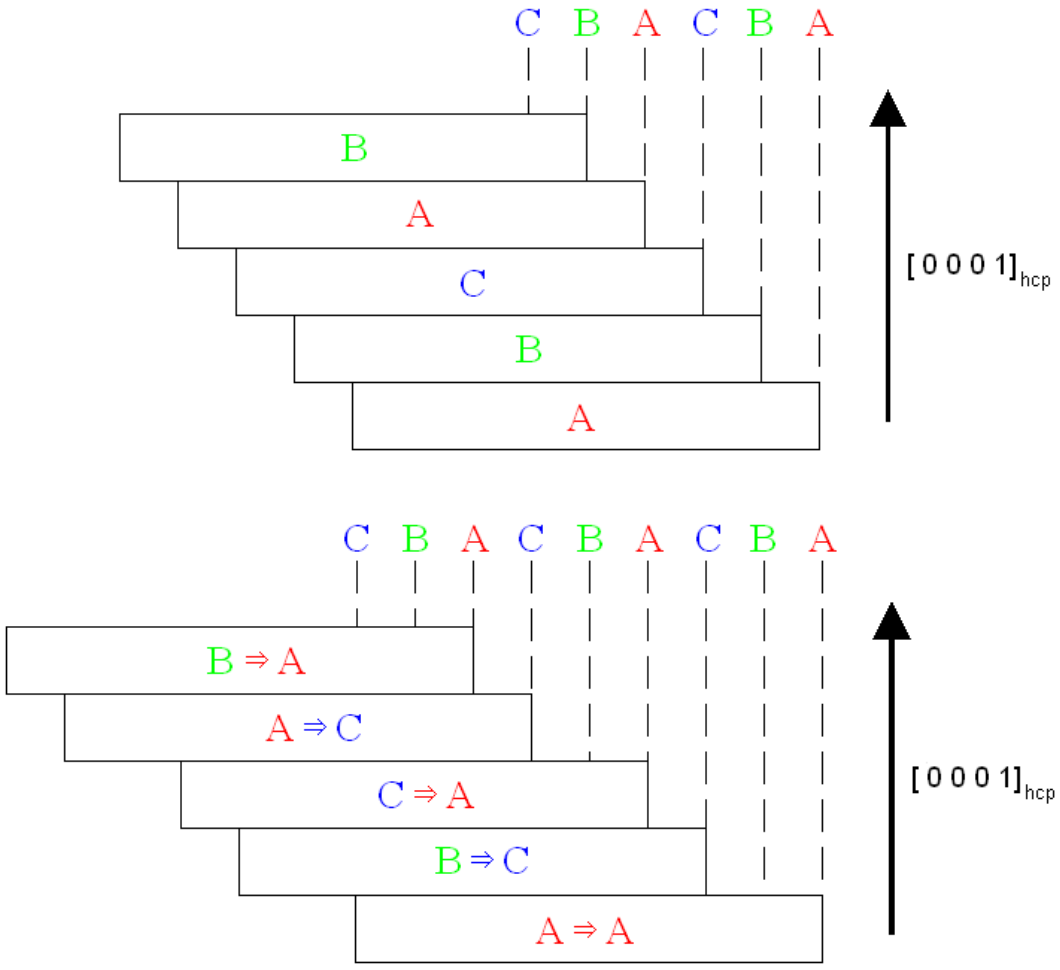

Pathway 468 Transition: First Group of Planes

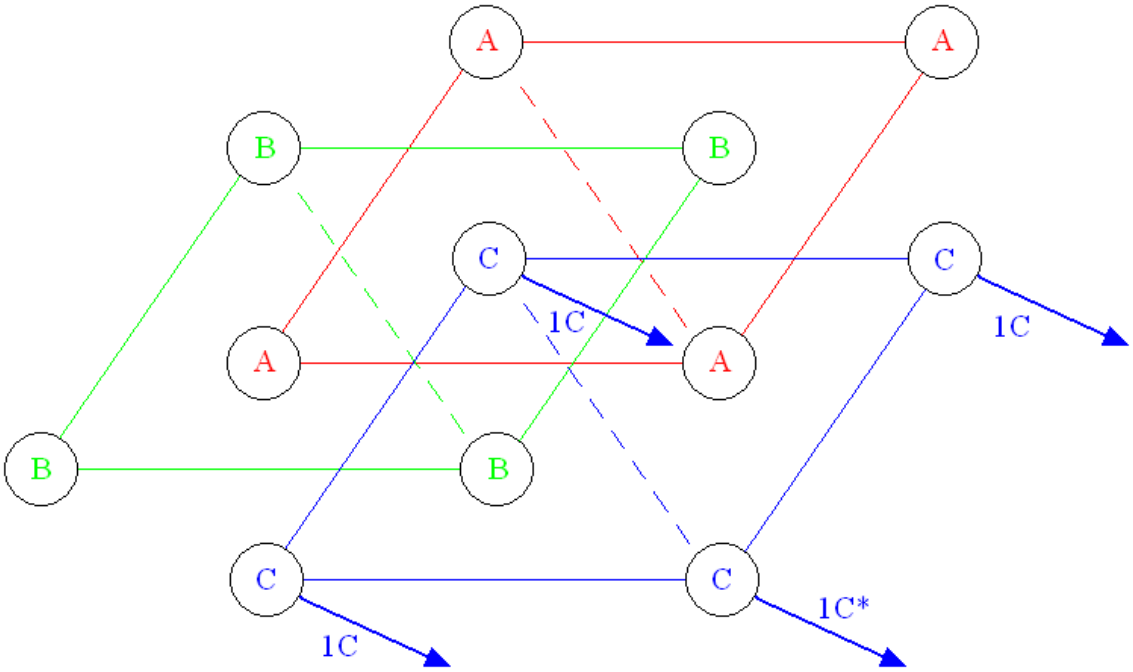

* = First C Plane

Pathway 468 Transition: Second Group of Planes

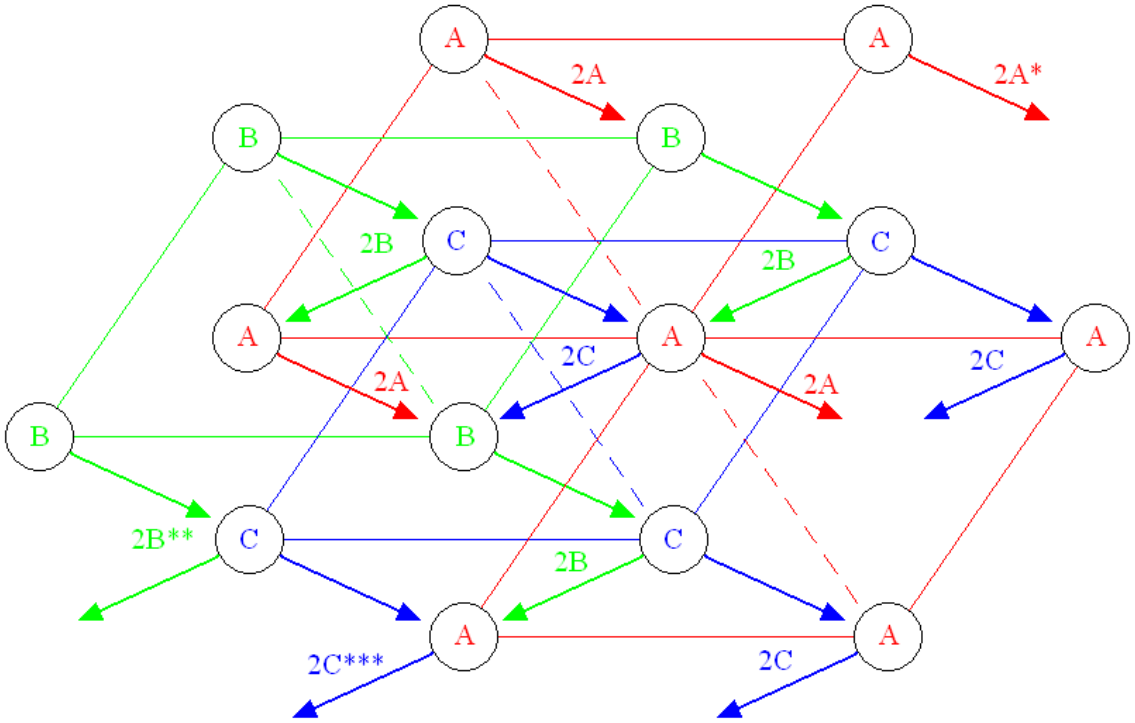

* = Second A Plane
** = Second B Plane
*** = Second C Plane

Pathway 468 Transition

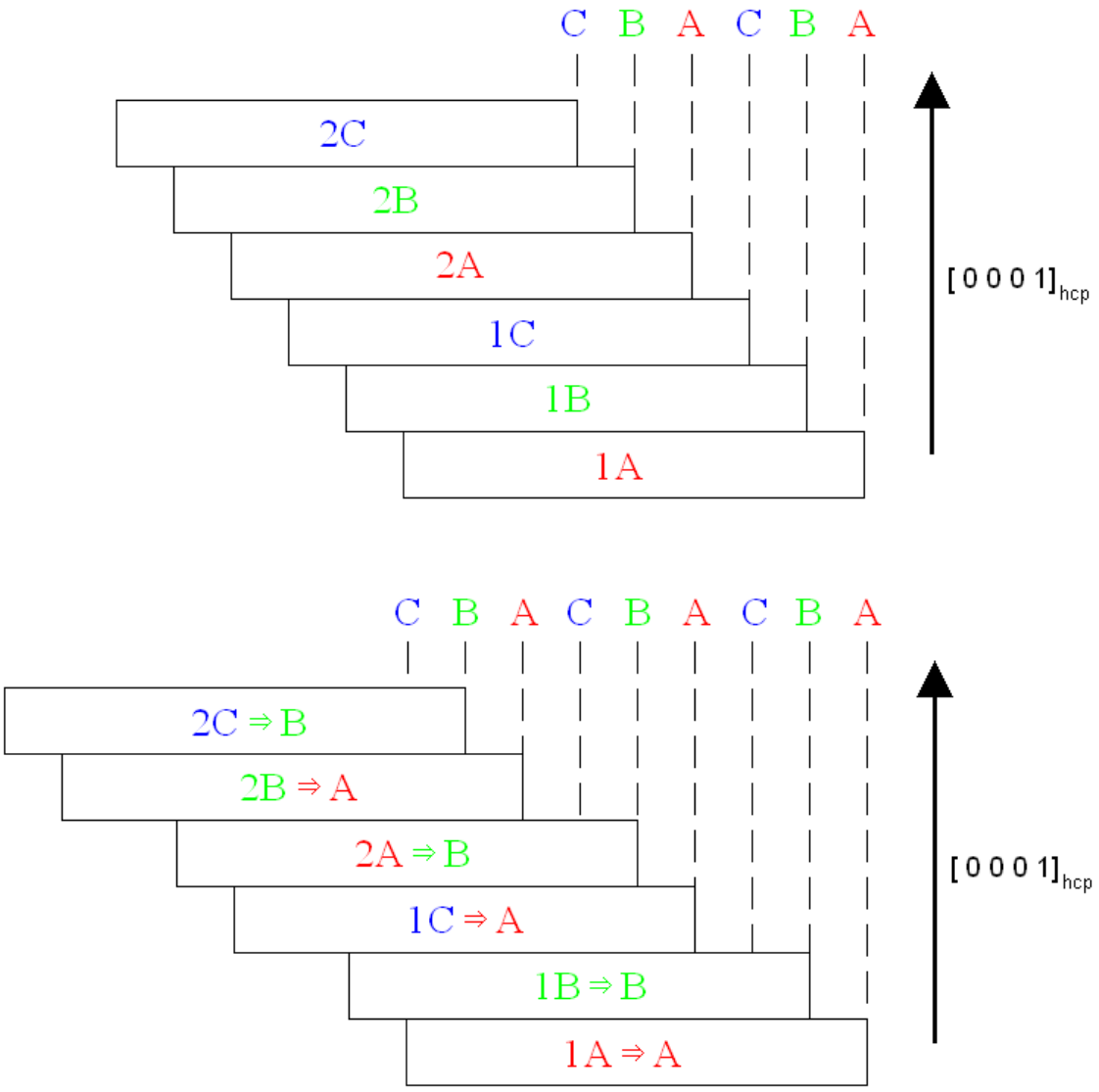

End Notes

[1]Amy Y. Liu, Alberto Garcia, Marvin L. Cohen, B. K. Godwal, and Raymond Jeanloz, Physical Review B. 43, 1795 (1991).

[2]Craig A. Vanderborgh, Yogesh K. Vohra, Hui Xia, and Arthur L. Ruoff, Physical Review B. 41, 7338 (1990).

[3]V. P. Dmitirev and S. B. Rochal, Physical Review Letters. 62, 2495 (1989)

[4]Ian Folkins and M. B. Walker, Physical Review Letters. 65, 127 (1990).

[5]Renata M. Wentzcovitch and Pui K. Lam, Third Series. 44, 9155 (1991).

[6]D. R. Trinkle, D. M. Hatch, H. T. Stokes, R. G. Hennig, and R. C. Albers, Physical Review B. 72, 014105 (2005).

[7]H. T. Stokes and D. M. Hatch, Physical Review B. 65, 144114 (2002).

[8]H. T. Stokes, D. M. Hatch, J. Dong, and J. P. Lewis, Physical Review B. 69, 174111 (2004).

[9]D. M Hatch, H. T. Stokes, J. Dong, J. Gunter, H. Wang, and J. P. Lewis, Physical Review B. 71, 184109 (2005).

[10]J. P Lewis, K. R. Glaesemann, G. A. Voth, J. Fritsch, A. A. Demkov, J. Ortega, and O. F. Sankey, Physics Review B. 64, 195103 (2001).

[11]H. T. Stokes and D. M. Hatch, Physical Review B. 65, 144114 (2002).

[12]http://stokes.byu.edu/comsubs.html

[13]D. M Hatch, H. T. Stokes, J. Dong, J. Gunter, H. Wang, and J. P. Lewis, Physical Review B. 71, 184109 (2005).